

Article

Experimental Study on the Dynamic Modulus of an Asphalt Roadbed Grouting Mixture under the Influence of Complex and Multiple Factors

Wuping Ran ¹, Hengzheng Qiu ^{2,*}, Xianchen Ai ¹, Shanshan Zhang ³ and Yaqiang Wang ²¹ School of Traffic and Transportation Engineering, Xinjiang University, Urumqi 830017, China² Xinjiang Civil Engineering Technology Research Center, Xinjiang University, Urumqi 830047, China³ College of Hydraulic and Architectural Engineering, Tarim University, Aral 843300, China

* Correspondence: wgywyx@163.com

Abstract: After long-term service, the ground will experience settlement and the stability of the roadbed will be lost. In order to effectively reinforce the roadbed, an asphalt roadbed grouting mixture has been applied to the filling of the roadbed. The rotary compaction method was used to prepare different gradation types of lime composite-modified oil sludge pyrolysis residue asphalt mixtures Sup13, Sup19, and Sup25. This article takes the dynamic modulus of an asphalt roadbed grouting mixture as the mechanical index, and the uniaxial compression dynamic modulus test is carried out on three kinds of rotary compaction asphalt mixtures, Sup13, Sup19, and Sup25. The dynamic modulus master curves of different gradation composite-modified oil sludge pyrolysis residue asphalt mixtures are fitted to study the dynamic modulus of asphalt mixtures under different nominal maximum particle sizes, loading frequencies, and temperatures. The results show that (1) The dynamic modulus of different gradation composite-modified oil sludge pyrolysis residue asphalt mixtures increases with the decrease in temperature and the increase in frequency; (2) when other conditions are the same, the compound-modified asphalt mixture's dynamic modulus decreases significantly under low-frequency and high-temperature conditions; (3) in the range of 4.4–37.8 °C and medium loading frequency, the dynamic modulus of the compound-modified asphalt mixture is more affected by temperature and loading frequency; (4) in the low-temperature and high-frequency range, the compound-modified asphalt mixture with a larger nominal maximum particle size has a higher dynamic modulus, and the asphalt mixture with better stability of skeleton structure has a higher dynamic modulus. The research results of this article will provide scientific guidance for the study of the mechanical properties of asphalt roadbed grouting mixtures.

Keywords: roadbed stability; land subsidence; asphalt grouting mixture; dynamic modulus; multiple factors



Citation: Ran, W.; Qiu, H.; Ai, X.; Zhang, S.; Wang, Y. Experimental Study on the Dynamic Modulus of an Asphalt Roadbed Grouting Mixture under the Influence of Complex and Multiple Factors. *Buildings* **2023**, *13*, 1969. <https://doi.org/10.3390/buildings13081969>

Academic Editors: Qingbiao Wang and Bin Gong

Received: 28 June 2023

Revised: 20 July 2023

Accepted: 27 July 2023

Published: 1 August 2023



Copyright: © 2023 by the authors. Licensee MDPI, Basel, Switzerland. This article is an open access article distributed under the terms and conditions of the Creative Commons Attribution (CC BY) license (<https://creativecommons.org/licenses/by/4.0/>).

1. Introduction

The karst development in the karst landform area is obvious, the formation instability is intensified, and the amount of land subsidence is large. The asphalt mixture can effectively improve the stability of the subgrade in the complex land subsidence area of the karst. One hot spot in academic research is how to realize the rational development of non-renewable resources such as coal and oil and apply its ancillary products to asphalt mixture [1–3]. In recent years, the number of oily solid waste sludge produced by oil exploitation has also increased rapidly, resulting in social and environmental problems such as large processing capacity and low resource utilization [4,5]. How to realize the resource utilization and disposal of oil sludge has become an urgent problem to be solved.

In oil sludge treatment technology, pyrolysis has the advantages of complete treatment, oil and gas resource recovery, heavy metal solidification in sludge, and less pollutant gas emission, and it is considered to be the most promising sludge treatment technology [6,7].

Microscopic analysis techniques such as SEM image processing technology and XRD analysis have been widely used, dramatically improving the accuracy of analyzing the internal microstructure distribution and chemical composition of materials [8–11]. Domestic and foreign scholars at home and abroad have found that the pyrolysis residue of oil sludge has a developed pore structure, rough surface, large specific surface area, and strong adsorption capacity [12,13]. Similar to the chemical composition of subgrade materials, it has broad application prospects in subgrade materials [14].

The pyrolysis residue of oil sludge has an abundant pore structure and strong physical adsorption characteristics. An alkaline solution can further improve the specific surface area of pyrolysis residue and enhance its adsorption capacity [15]. Vaisman et al. [16] used a water washing method to treat oil sludge pyrolysis residue instead of mineral powder to prepare the asphalt mixture, which can meet the requirements of road performance in some areas. Mo et al. [17] used FT-IR and TG-DTG to analyze the functional group characteristics of oil sludge pyrolysis residue and found that the pyrolysis residue contained a large number of organic functional groups similar to asphaltene. Albayatia et al. [18] found that hydrated lime can adsorb clay particles on the surface of aggregate and reduce the influence of uncarbonized clay particles in the pyrolysis residue of oil sludge on the bonding performance of asphalt. Zhu [19] found that the hydrocarbons and hydroxyl compounds in the pyrolysis residue of oil sludge were integrated into the asphalt, which had a specific absorption effect on the light components in the asphalt, enriched the components of the asphalt, and increased the adhesion between the asphalt mortar and the aggregate. Cong Lin et al. [20] analyzed that the asphalt mixture containing 4% clay can significantly improve the water stability of the asphalt mixture after adding an appropriate amount of lime.

As a typical viscoelastic material, the mechanical response of asphalt mixtures is characterized by a dynamic shift in the actual use process. The dynamic modulus can comprehensively reflect the stress and strain characteristics of materials under dynamic load and asphalt temperature characteristics, which is an essential parameter for the structural design of asphalt pavement [21,22]. At present, domestic and foreign scholars use the time–temperature equivalence principle and the Sigmoidal mathematical model to draw the dynamic modulus master curve, and use the W.L.F equation to calculate the shift factor to obtain the dynamic modulus characteristics of asphalt mixture in a wider temperature range and a wider frequency range [23]. In addition, different scholars have studied the variation of dynamic modulus with temperature and frequency for modified asphalt mixtures with other materials, analyzed the dynamic mechanical response of mixtures at different temperatures and load frequencies, and explored the stress–strain characteristics of materials in different environments [24,25].

At present, there needs to be more systematic research on the application of composite-modified oil sludge pyrolysis residue asphalt mixture in road engineering. This study used lime composite-modified oil sludge pyrolysis residue to replace the mineral powder to design a composite-modified oil sludge pyrolysis residue asphalt mixture. The gradation design of Sup13, Sup19, and Sup25, three groups of composite-modified oil sludge pyrolysis residue asphalt mixtures, was carried out. The Superpave method was used to determine the optimum oil–stone ratio of the mixture. The asphalt mixture specimen was formed by the rotary compaction method. The dynamic modulus of composite-modified oil sludge pyrolysis residue asphalt mixture was studied by the uniaxial compression dynamic modulus test. Based on the results of the dynamic modulus test, the master curve of the dynamic modulus of asphalt mixture with composite-modified oil sludge pyrolysis residue was obtained by using the principle of time–temperature equivalence. The stress–strain characteristics of asphalt mixture under a wide temperature range and significant frequency was analyzed, which provided the reference for applying oil sludge pyrolysis residue in road engineering.

2. Materials and Test Scheme

2.1. Basic Properties of Materials

2.1.1. Asphalt

In this paper, Xinjiang Karamay AH-90 # asphalt provided by a company in Xinjiang, is selected. The test method is referred to ‘Standard Test Methods of Bitumen and Bituminous Mixtures for Highway Engineering’ (JTG E20-2011) [26]. The main performance indicators are shown in Table 1.

Table 1. Main specifications of Xinjiang Karamay AH-90 # matrix asphalt.

Technology Specifications	Test Value	Quality Indicator	Testing Method
Needle penetration (25 °C, 100 g, 0.1 mm)	84	80~100	T0604-2011
Needle penetration index PI	−1.02	−1.5~+1.0	T0604-2011
Softening point (universal method)/°C	46.0	≥45	T0606-2011
Power Viscosity (60 °C) Pa·s	178	≥160	T0620-2000
Latency (15 °C, 5 cm/min, cm)	>100	≥100	T0605-2011
Latency (10 °C, 5 cm/min, cm)	>100	≥100	T0605-2011
Wax content (distillation method)%	1.9	≤2.2	T0615-2011
Flash point (open) °C	>300	≥245	T0611-2011
Solubility (trichloroethylene)/°C	99.84	≥99.5	T0607-2011
Density (15 °C), g/cm ³	0.982	Real value	T0603-2011
Quality changes	−0.112	−0.8~+0.8	T0609-2011
TFOR (or RTFOT) residues	Residual needle penetration ratio, %	62.4	≥61
	Residual ductility ratio (10 °C)/cm	11.9	≥6

2.1.2. Oil Sludge Pyrolysis Residue and Lime

The pyrolysis residue of oil sludge is affected by factors such as crude oil type and final pyrolysis temperature, and its physical and chemical properties are different [27]. The pyrolysis residue of oil sludge used in this paper is taken from a company in Xinjiang, and its pyrolysis process is shown in Figure 1.

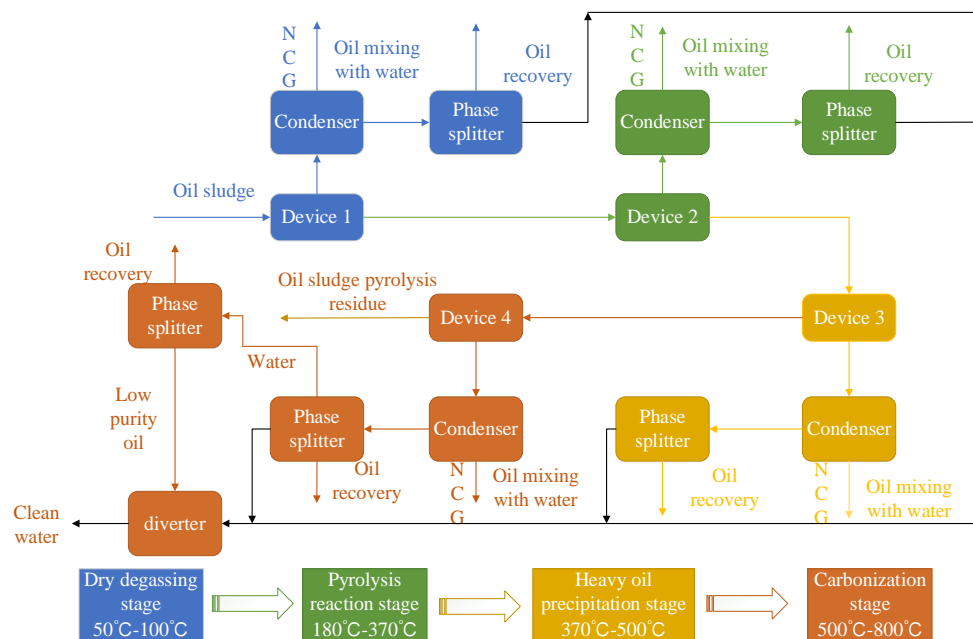


Figure 1. Oil sludge pyrolysis process.

In order to analyze the microstructure characteristics of oil sludge pyrolysis residue, the microstructure of the material was scanned by a scanning electron microscope (SEM), and the results are shown in Figure 2.

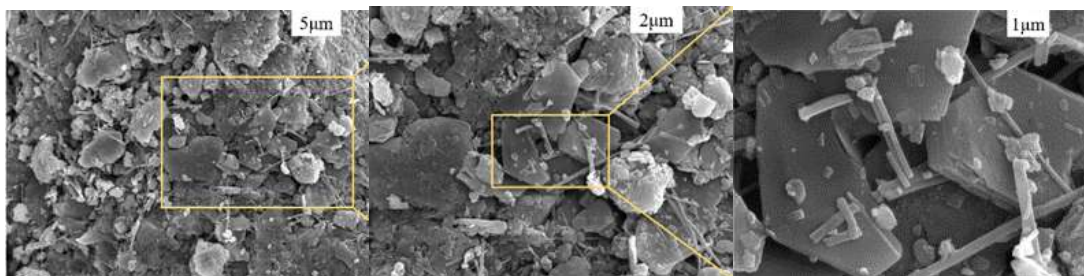


Figure 2. Scanning electron microscope results of pyrolysis residue.

It can be seen from Figure 2 that the microstructure of the pyrolysis residue of oil sludge shows a large number of rod-like structures and porous structures. There are a large number of folds and bulges on the material's surface, which increases the contact area with the asphalt. When the asphalt is in contact with the pyrolysis residue of oil sludge, the tiny molecules or oil with a short molecular chain in the asphalt will immerse into the gap, showing an excellent liquid phase diffusion effect, which is conducive to the absorption of organic macromolecules by the pyrolysis residue of oil sludge, and creates an excellent physical condition for selective absorption with asphalt.

The research treated the pyrolysis residue of oil sludge and lime and determined the material's physical properties. The test method refers to the 'Test Method of Aggregate for Highway Engineering' (JTG E42-2005) [28], and the test results are shown in Tables 2 and 3.

Table 2. Main technical specifications of mineral powder and oil sludge pyrolysis residue [29].

Technology Specifications	Limestone Powder	Oil Sludge Pyrolysis Residue	Testing Method
Density (g/cm ³)	2.71	2.57	T0352-2000
Hydrophilic coefficient	0.82	0.79	T0353-2000
Specific surface area (m ² /g)	0.587	0.813	T8074-2008

Table 3. Main technical indexes of lime [29].

Performance Index	Measured Value	Quality Index	Testing Method
Ca and Mg content(%)	78.1	≥60	EDTA
Percentage of moisture(%)	1.9	<4	T0103
Density (g/cm ³)	2.543	Measured value	T0352-2000

2.1.3. Aggregate

This paper provides aggregates from a company in Xinjiang, where the coarse aggregates are basaltic and the fine aggregates are limestone. According to the 'Test Method of Aggregate for Highway Engineering' (JTG E42-2005) [28], the aggregate property test was carried out, and all the properties met the requirements. The test results for the main technical metrics of the aggregate are shown in Table 4.

Table 4. Main performance indexes of aggregate.

Particle Size (mm)	Apparent Density (g/cm ³)	Table Dry Density (g/cm ³)	Bulk Volume Density (g/cm ³)	Water Absorption (%)
26.5	2.663	2.645	2.634	0.41
19	2.666	2.648	2.637	0.41
16	2.692	2.676	2.666	0.37
13.2	2.661	2.644	2.635	0.37
9.5	2.693	2.674	2.663	0.41
4.75	2.695	2.670	2.654	0.57
2.36	2.682	2.625	2.592	1.29
1.18	2.786	2.655	2.582	2.82
0.6	2.744	2.684	2.650	1.28
0.3	2.666	2.591	2.546	1.76
0.15	2.637	2.597	2.573	0.94
0.075	2.735	-	-	-

2.2. Test Materials and Methods

2.2.1. Determine Gradation

The materials used in the existing road structure are analyzed, and three gradations of Superpave13, Superpave19, and Superpave25 are selected for gradation design. Each gradation is designed into three sets, A, B, and C. Figure 3 shows the gradation design curves for different nominal maximum particle sizes.

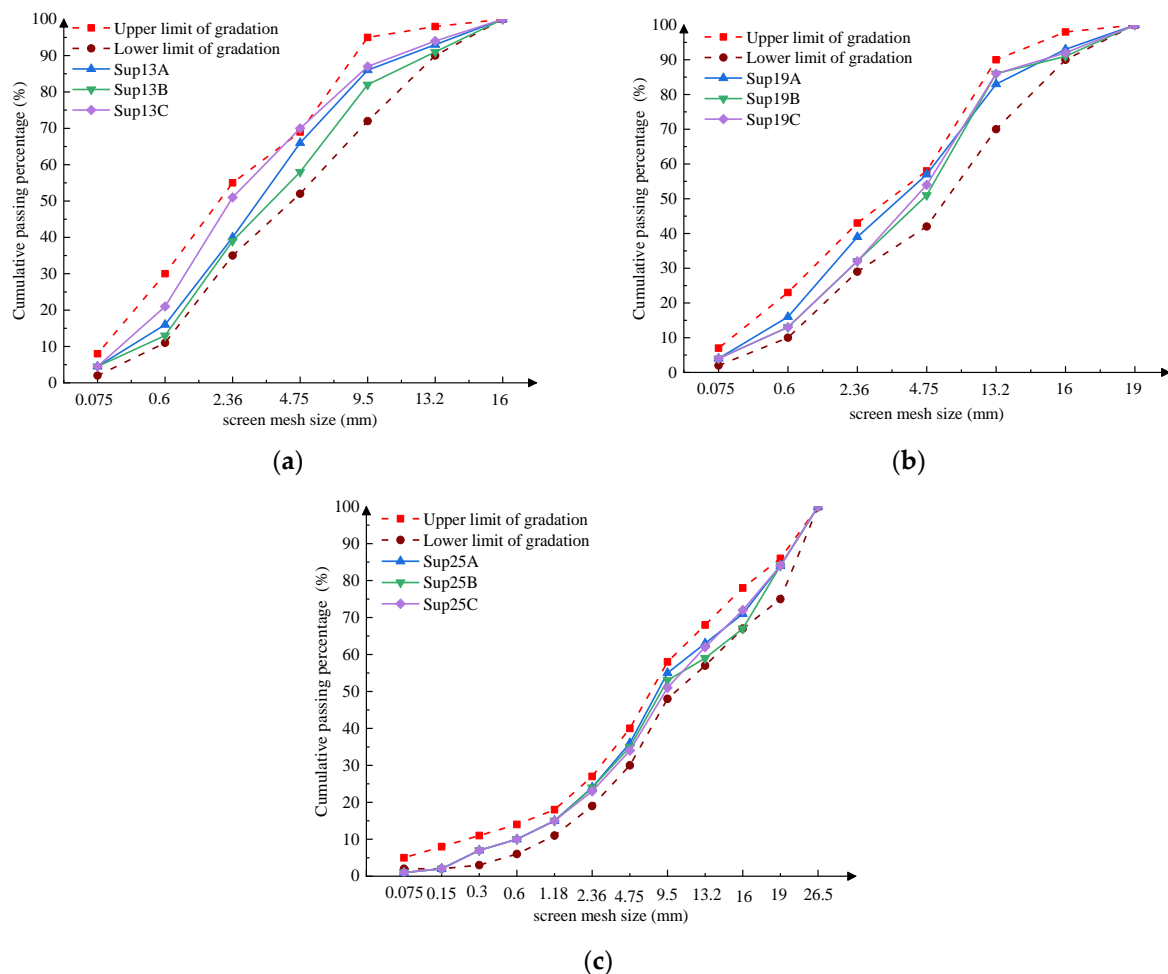


Figure 3. Superpave gradation design curve. (a) Superpave13 gradation design curve; (b) Superpave19 gradation design curve; (c) Superpave25 gradation design curve.

The different graduations of the asphalt mixture were mixed at the beginning, and the pressure test was used to obtain the different graduations of the gyratory compaction curves, as shown in Figure 4.

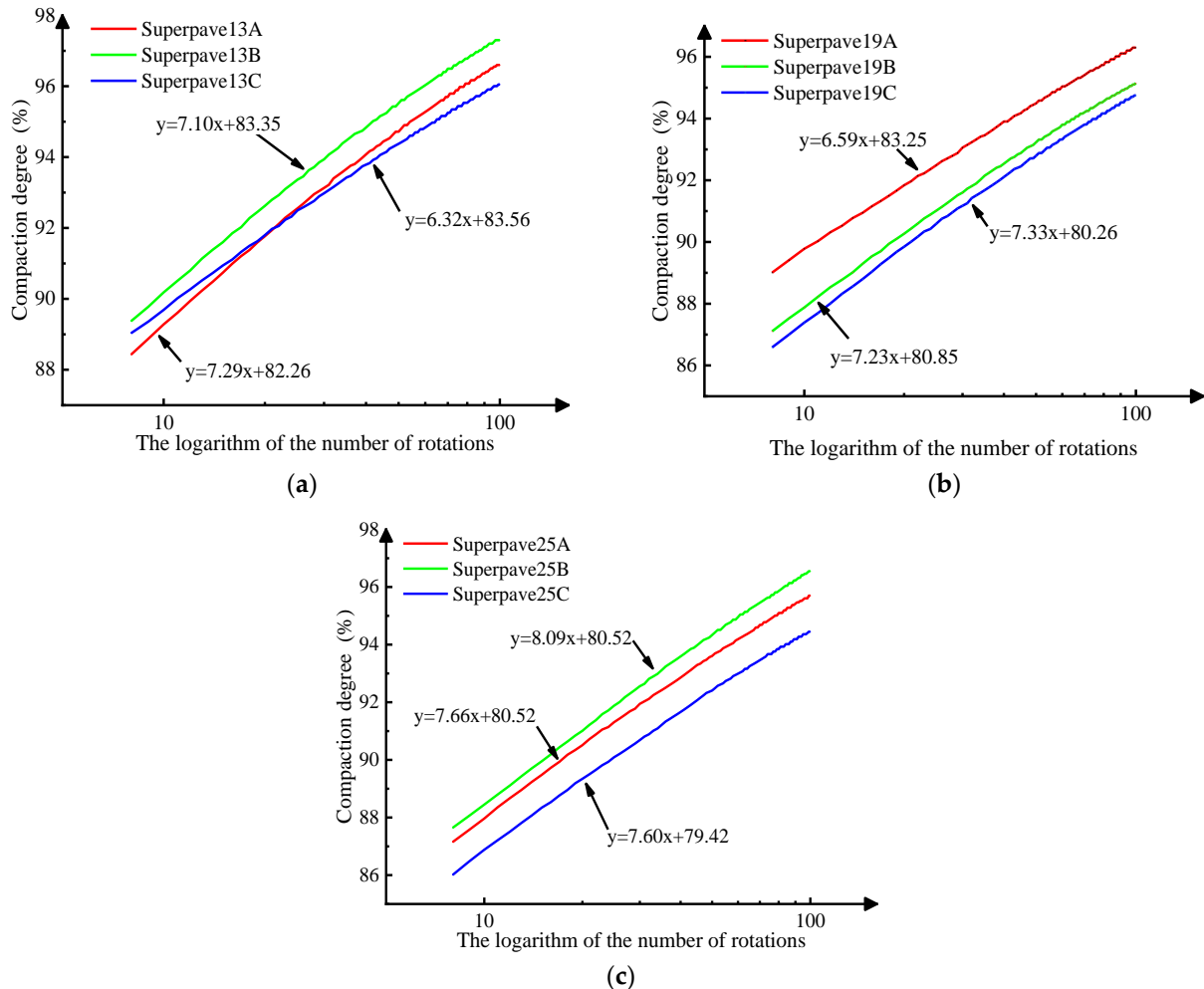


Figure 4. Rotary compaction characteristic curve. (a) Superpave13 rotary compaction characteristic curve; (b) Superpave19 rotary compaction characteristic curve; (c) Superpave25 rotary compaction characteristic curve.

The greater the slope of the rotary compaction characteristic curve, the greater the structural strength of the asphalt mixture and the better the stability of the asphalt mixture. It can be seen from Figure 4 that the optimal design graduations of three groups of asphalt mixtures with different nominal maximum particle sizes are Superpave13A, Superpave19C, and Superpave25B, respectively. According to the above three kinds of gradation mixture porosity, mineral aggregate gap rate, asphalt filling rate, the initial compaction conditions of mixture compaction degree, and other volume parameters, to obtain three groups of gradation optimum asphalt content. Figure 5 shows the relevant index parameters of the asphalt mixture.

Figure 5 shows that each optimal asphalt content satisfies both the Superpave volume index and compactness requirements. Moreover, the degree of compaction is less than 98 percent at the maximum number of compacts. Finally, the Sup13A grade has an optimum asphalt content of 4.48%. Sup19C has an optimum asphalt content of 4.41%. The Sup25B grade has an optimum asphalt content of 3.96 percent.

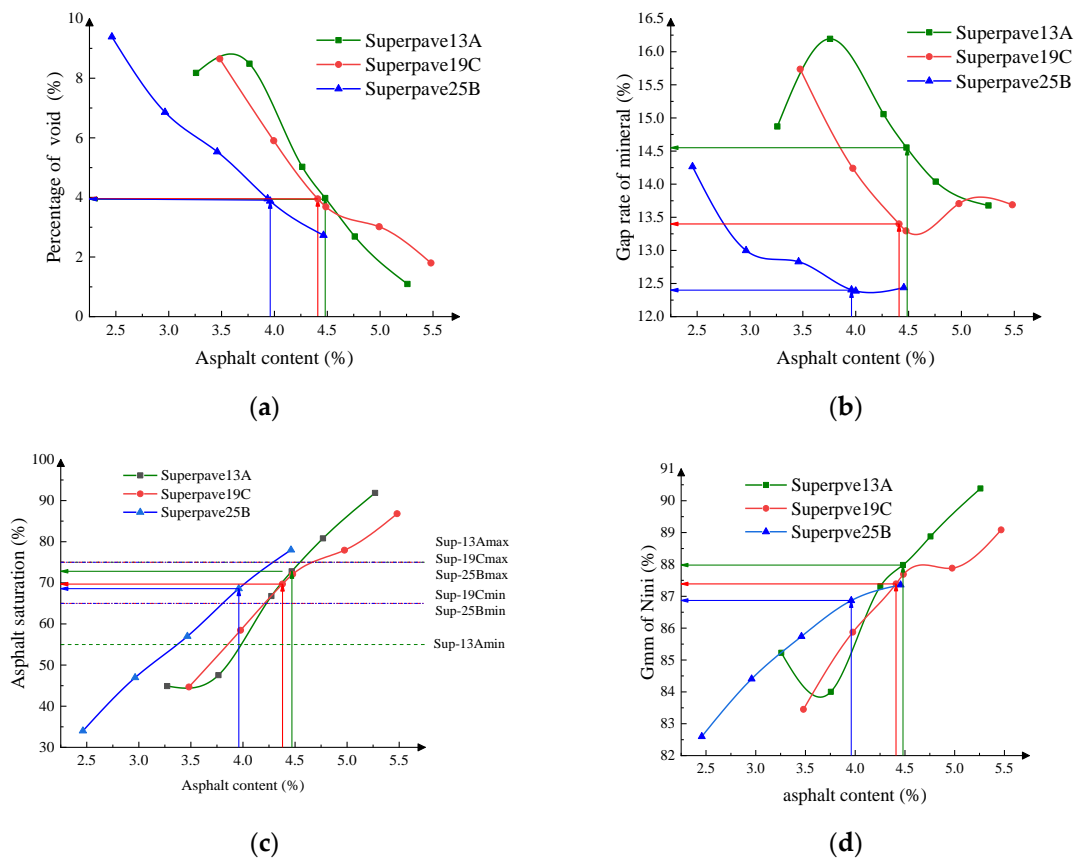


Figure 5. Change in asphalt mixture volume index with asphalt content. (a) The influence of asphalt content on V_a ; (b) the influence of asphalt content on VMA; (c) the influence of asphalt content on VFA; (d) the influence of asphalt content on the compaction degree of the mixture under N_{ini} .

2.2.2. Test Method

The main test methods of existing research include numerical simulation, laboratory tests, field tests, and other methods, and extensive research has been carried out on material properties and evolution mechanisms [30–32]. Comprehensive comparison of various research methods, the indoor test can accurately reflect the material properties and has good economic benefits. This paper uses the indoor test method to study the dynamic mechanical response of modified oil sludge pyrolysis residue modified asphalt mixture with different gradations, which provides a reference for the subsequent engineering application of materials. Existing studies have pointed out that when the lime content is 30%, the high-temperature, low-temperature, water sensitivity, and other comprehensive performances of asphalt mortar are the best [19]. In order to improve the modification effect of hydrated lime, hydrated lime with a filler mass fraction of 30% and oil sludge pyrolysis residue were selected to form a filler to react entirely and then mixed with asphalt to make an asphalt mortar. According to the optimum asphalt content determined in the previous section, the rotary compaction method formed different gradation types of asphalt mixtures. According to the above three groups of different nominal maximum particle size gradations, the mixture specimens were formed by the rotary compaction molding method. The test temperatures were $-10\text{ }^{\circ}\text{C}$, $4.4\text{ }^{\circ}\text{C}$, $21.1\text{ }^{\circ}\text{C}$, $37.8\text{ }^{\circ}\text{C}$, and $54.4\text{ }^{\circ}\text{C}$, and the loading frequencies were 25 Hz, 10 Hz, 5 Hz, 1 Hz, 0.5 Hz, and 0.1 Hz, respectively. The UTM-130 asphalt mixture test system was used to measure the dynamic modulus of the composite-modified oil sludge pyrolysis residue mixture at different temperatures and load frequencies. The standard specimen after core cutting is shown in Figure 6, and the specimen before loading is shown in Figure 7.



Figure 6. Standard specimen after core cutting.



Figure 7. The specimen before loading.

3. Results and discussion

3.1. Dynamic Modulus Test Results and Analysis

Asphalt mixture is a typical viscoelastic material with apparent time and temperature dependence. The dynamic modulus test can be used to study the dynamic mechanical response of the asphalt mixture under different temperatures and loading frequencies. The dynamic modulus of the asphalt mixture can be calculated by applying a certain period and waveform dynamic load to the material. The calculation formula is shown in Equations (1)–(3).

$$\sigma_0 = \frac{P_i}{A} \quad (1)$$

$$\varepsilon_0 = \frac{\Delta_i}{l_0} \quad (2)$$

$$|E^*| = \frac{\sigma_0}{\varepsilon_0} \quad (3)$$

In the equation:

P_i —The average amplitude of the axial test load in the last five loading cycles (N),

A —The average area of the upper and lower ends of the specimen (mm^2),

Δ_i —The average amplitude of recoverable axial deformation in the last five loading cycles is recovered (mm),

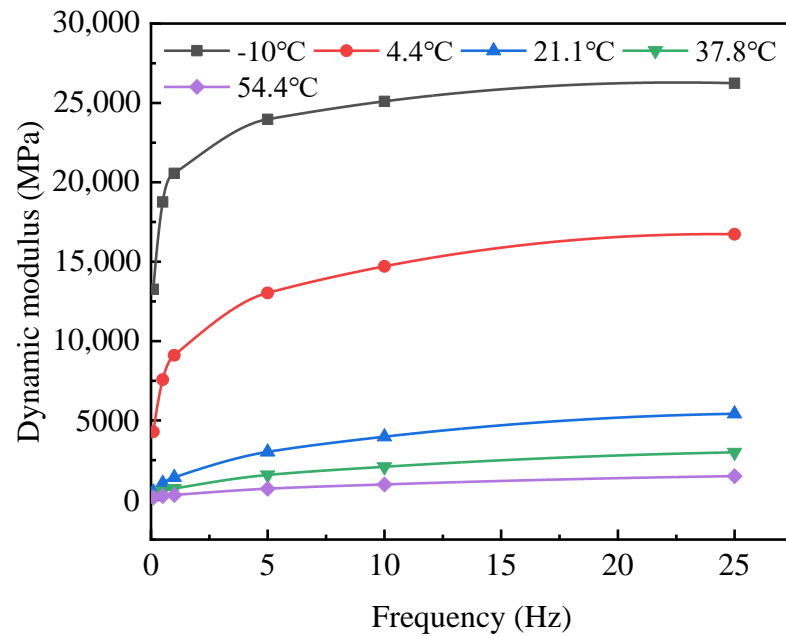
l_0 —The measurement spacing of sensors on the upper part of the specimen (mm)

σ_0 —Axial stress amplitude (MPa),

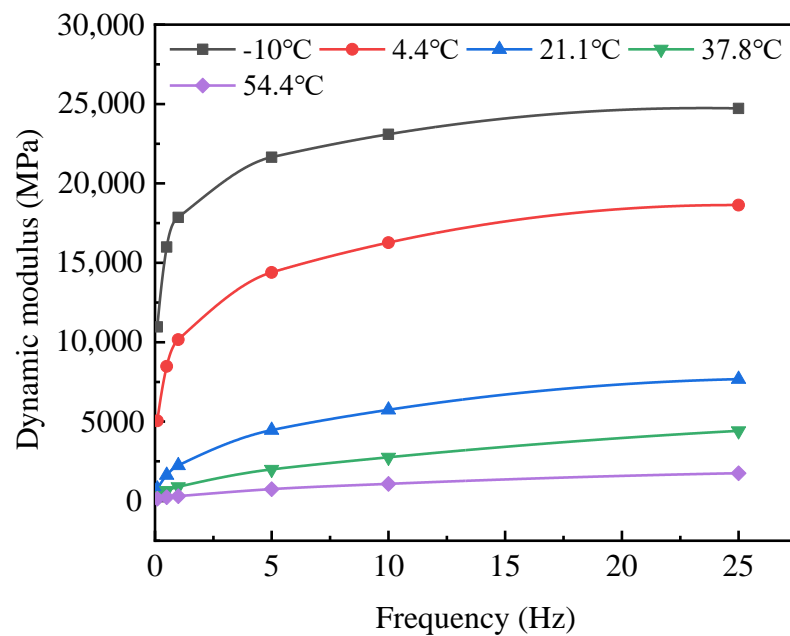
ε_0 —Axial strain amplitude value (mm/mm), and

$|E^*|$ —Dynamic modulus of asphalt mixture (MPa).

Calculating the dynamic modulus of three kinds of composite-modified oil sludge pyrolysis residue asphalt mixture under different test conditions. The results are shown in Figure 8.

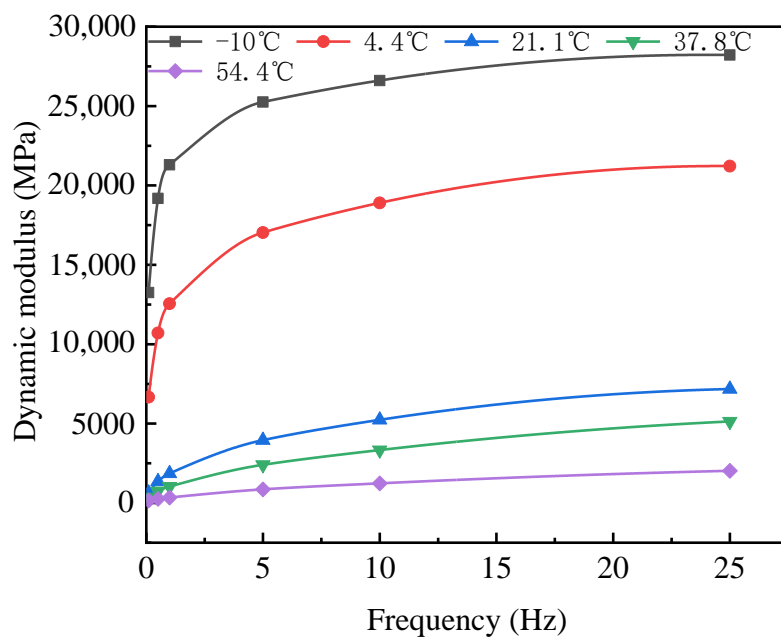


(a)



(b)

Figure 8. Cont.



(c)

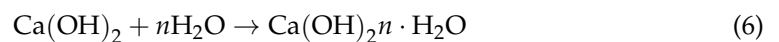
Figure 8. Dynamic modulus of composite-modified oil sludge pyrolysis residue asphalt mixtures. (a) Sup13 dynamic modulus of composite-modified oil sludge pyrolysis residue asphalt mixtures; (b) Sup19 dynamic modulus of composite-modified oil sludge pyrolysis residue asphalt mixtures; (c) Sup25 dynamic modulus of composite-modified oil sludge pyrolysis residue asphalt mixtures.

As seen from Figure 8, the dynamic modulus of the composite-modified oil sludge pyrolysis residual asphalt mixture with different graduations decreases with increasing temperature and increases with increasing frequency. The dynamic modulus of the material decreases significantly under high temperature and low-frequency conditions. The dynamic modulus at 25 Hz at $-10\text{ }^{\circ}\text{C}$ is only approximately two fold that at 0.1 Hz, while the dynamic modulus at 25 Hz at $54.4\text{ }^{\circ}\text{C}$ is approximately 10~13 fold that at 0.1 Hz. When the frequency is 25 Hz, the dynamic modulus of asphalt mixture at $-10\text{ }^{\circ}\text{C}$ is approximately 14~18 fold that at $54.4\text{ }^{\circ}\text{C}$. When the frequency is 0.1 Hz, the dynamic modulus of asphalt mixture at $-10\text{ }^{\circ}\text{C}$ is approximately 76~87 fold that at $54.4\text{ }^{\circ}\text{C}$.

The temperature mainly affects the properties of the asphalt. In the range of $-10\text{--}54\text{ }^{\circ}\text{C}$, as the temperature increases, the penetration of asphalt increases, and the high-temperature stability of the mixture decreases. It is more prone to deformation under external action, and the dynamic modulus decreases. When the loading frequency becomes larger in a specific frequency range, the viscoelastic properties affect the asphalt mixture to produce a lag effect. The larger the loading frequency, the smaller the strain generated by the asphalt mixture, and the greater the dynamic modulus obtained by the test.

The composite-modified oil sludge pyrolysis residue asphalt mortar exhibits different viscoelastic characteristics at different temperatures. There are different adhesion properties between asphalt and aggregate, and the dynamic mechanical response of the material is different. As an alkaline modified material, hydrated lime has a specific activation effect on pyrolysis residue [33], which can increase the contact area with asphalt, form a more stable mortar material, and improve the adhesion state between asphalt and aggregate. Ca^{2+} can react with the clay particles in the pyrolysis residue to form stable calcium salt particles, which can improve the flexibility of asphalt mortar and the dynamic modulus of asphalt mixture at low temperatures [34]. The calcium ion in the crystal formed by the self-crystallization of lime can react with the polar carboxyl group in the asphalt to improve the high temperature performance and adhesion performance of the asphalt mortar and improve the dynamic modulus of the material at high temperature [35,36]. Under the

combined action of physical adsorption and chemical adsorption between the pyrolysis residue of oil sludge modified by hydrated lime and asphalt, the bonding force between asphalt mortar and aggregate is improved, the rheological properties of asphalt mortar are improved, and the dynamic modulus of asphalt mixture with composite-modified pyrolysis residue of oil sludge is improved. The reaction equation of lime and residue and the self-crystallization reaction equation of lime are shown in Equations (4)–(6).



3.2. Dynamic Modulus Master Curve

Existing studies have pointed out that the viscoelastic behavior of asphalt materials is equivalent at higher temperatures and higher frequencies and can be converted to each other to determine a larger loading frequency range and a wider temperature and dynamic modulus of asphalt mixture [37]. Based on the time–temperature equivalence principle, this paper establishes the master curve of the dynamic modulus of three graded mixtures. Furthermore, it analyzes and compares the influence of different nominal maximum particle sizes, temperature, loading frequency, and other factors on the dynamic modulus of the mixture.

This paper uses the Sigmoidal mathematical model to fit the dynamic modulus master curve of the asphalt mixture. The expression is shown in Equation (7) [38].

$$\lg|E^*| = \delta + \frac{\alpha}{1 + e^{\beta + \gamma(\lg\omega_\gamma)}} \quad (7)$$

In the equation: $|E^*|$ is the dynamic modulus of asphalt mixture (MPa), δ , α , β , γ are model regression coefficients, $\delta + \alpha$ is the maximum dynamic modulus, where δ is the minimum dynamic modulus, β , γ are Sigmoidal function shape parameters, ω_γ is the reduced frequency.

The functional relationship between dynamic modulus and loading frequency of asphalt mixture at the reference temperature is determined by the Sigmoidal function. The shift factor is the distance from the dynamical modulus value to the reference temperature at different test temperatures. This paper uses the W.L.F. formula to calculate the shift factor. The expression is given in Equation (8).

$$\lg a_T = \frac{-C_1(T - T_g)}{C_2 + T - T_g} \quad (8)$$

In the equation:

a_T —shift factor, at reference temperature a_T is 1;

C_1, C_2 —constant, related to material properties;

T —Material test temperature ($^{\circ}\text{C}$);

T_g —The material reference temperature is generally the glass brittle point temperature of amorphous polymer ($^{\circ}\text{C}$).

According to the time–temperature equivalence principle, the shift factors at different temperatures were obtained by nonlinear least squares fitting. The planning solution method is used to fit the dynamic modulus data at different temperatures to obtain the master curve parameters of the asphalt mixture, and the goodness of fit is evaluated by the correlation coefficient R^2 . The master curve parameters and shift factors are shown in Tables 5 and 6, respectively. The master curve of the dynamic modulus of the asphalt mixture is shown in Figure 9.

Table 5. Master curve parameters of different gradation asphalt mixtures.

Grading Type	Regression Parameter				WLF Equation Parameters		R ²
	δ	α	β	γ	C ₁	C ₂	
Sup13	1.733	2.669	−0.265	−0.710	4.357	59.828	0.992
Sup19	1.557	2.893	−0.601	−0.688	7.861	109.861	0.994
Sup25	1.657	2.792	−0.539	−0.736	5.211	72.43	0.982

Table 6. Shift factor of different gradation asphalt mixtures.

Grading Type	Temperature (°C)				
	−10	4.4	21.1	37.8	54.4
Sup13	4.716	1.687	0	−0.951	−1.558
Sup19	3.104	1.409	0	−1.037	−1.828
Sup25	3.921	1.561	0	−0.976	−1.641

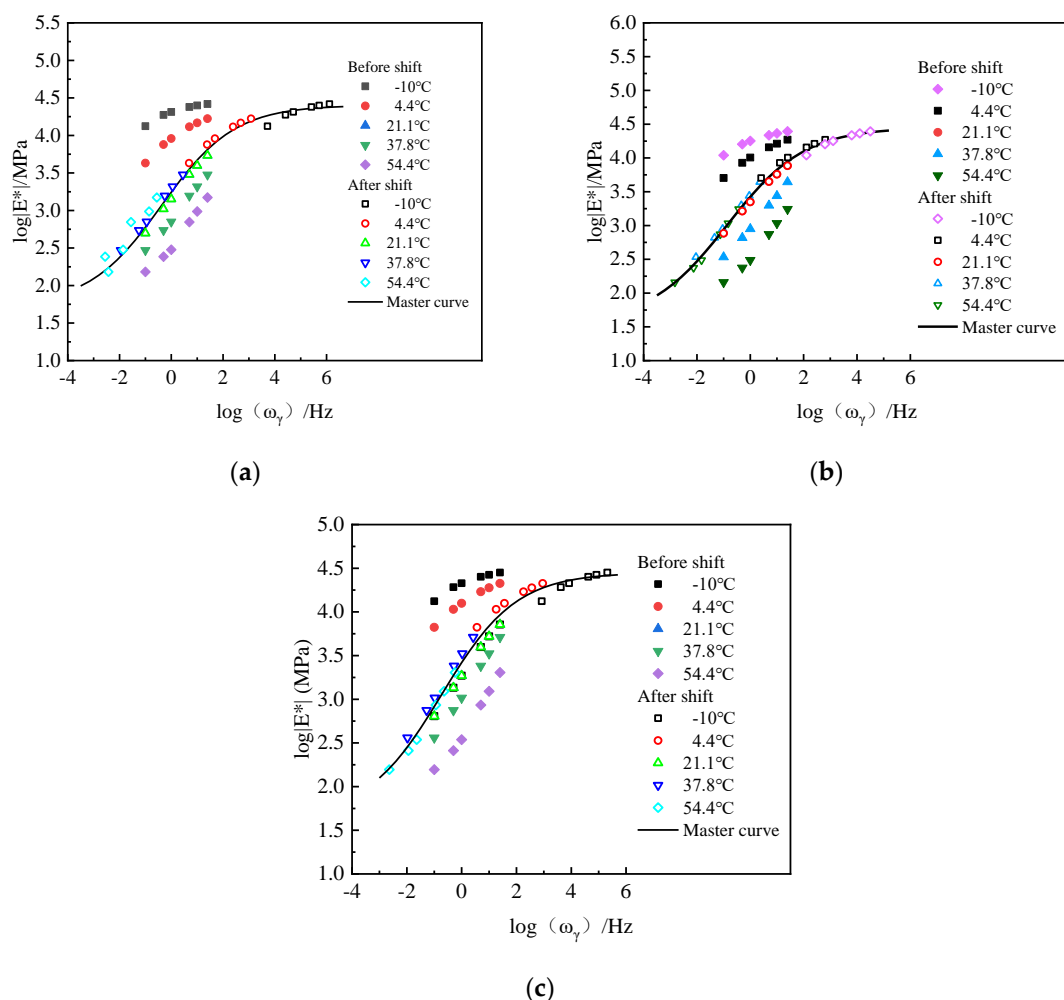
**Figure 9.** Master curve of Superpave asphalt mixtures. (a) Master curve of composite-modified oil sludge pyrolysis residue Superpave13 asphalt mixtures; (b) master curve of composite-modified oil sludge pyrolysis residue Superpave19 asphalt mixtures; (c) master curve of composite-modified oil sludge pyrolysis residue Superpave25 asphalt mixtures.

Table 5 and Figure 9 show that the master curve of dynamic modulus is S-shaped, the R² of each gradation fitting curve is greater than 98%, and the fitting curve has an excellent correlation with the test data. As shown in Figure 9, with the increase in loading

frequency, the dynamic modulus of each group increases. With the increase in temperature, the dynamic modulus of each group decreased. In addition, the dynamic modulus of the mixture is less affected by the loading frequency in the $-10\text{ }^{\circ}\text{C}$ and $54.4\text{ }^{\circ}\text{C}$ sections, and the master curve is gentle. In the range of $4.4\text{--}37.8\text{ }^{\circ}\text{C}$, the slope of the dynamic modulus master curve of the mixture is large, and the frequency significantly affects the dynamic modulus. When the loading frequency gradually changes from low to high, the slope of the master curve also shows a trend of increasing first and then decreasing. The dynamic modulus of the mixture is affected mainly by the frequency in a specific intermediate frequency range. It is less affected by the frequency in the extremely low or extremely high-frequency range.

The above dynamic modulus change trend comprehensively reflects the viscoelasticity of the asphalt mixture. When the temperature is low, the asphalt mixture shows prominent elastic properties. The stress–strain characteristics of the material are mainly affected by the internal skeleton structure of the mixture, and the slope of the master curve is slight. In the high-temperature section, the asphalt mixture mainly exhibits plastic characteristics. The modulus of the asphalt material decreases and is less affected by the temperature change. At this time, the dynamic modulus is less affected by the master curve, and the slope of the master curve is slight. In a specific intermediate temperature range, asphalt shows obvious viscoelasticity. At this time, the stress–strain characteristics of the mixture are largely affected by temperature, showing a sizeable master curve slope.

The change in loading frequency mainly affects the lag effect inside the mixture. When the frequency is shallow, the stress characteristics of the mixture are similar to the static load, the stress–strain characteristics show high consistency, and the hysteresis effect is insignificant. When the frequency is relatively high, the stress time of the mixture is very short, and the lag effect is small. Therefore, in the moderate frequency range, the stress–strain characteristics of the mixture show an intense lag, the dynamic modulus is considerably affected by the frequency, and the slope of the master curve is enormous.

As shown in Figure 10, there are differences between the master curves for different nominal maximum particle size mixtures. In the low-temperature and high-frequency section, the dynamic modulus of the Sup25-graded asphalt mixture is higher than that of the other two asphalt mixtures. In the high-temperature and low-frequency section, the dynamic modulus of the Sup25 gradation and Sup19 gradation asphalt mixture is similar, and the dynamic modulus of the Sup13 gradation asphalt mixture is the smallest. The mixture with larger nominal particle size shows higher dynamic modulus in different temperature and frequency ranges. It shows that the stress–strain characteristics of the mixture are also affected by the gradation of the mixture. Due to the excellent stability of the skeleton structure, a dense skeleton mixture is better able to resist the effects of the external environment and has a higher dynamic modulus.

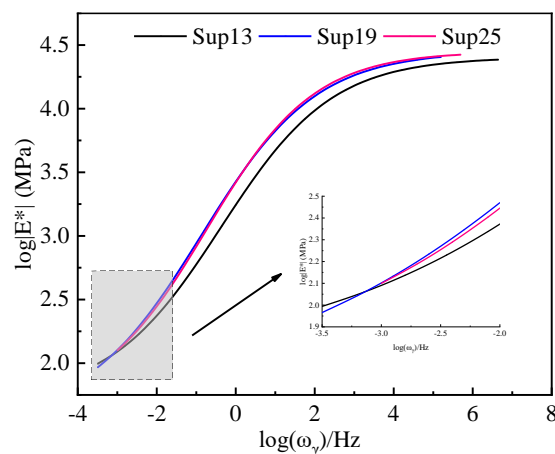


Figure 10. Master curve of dynamic modulus of asphalt mixture with different gradations.

4. Conclusions

The rotary compaction method was used to prepare three kinds of asphalt mixtures, Superpave13, Superpave19, and Superpave25, of oil sludge pyrolysis residue asphalt mixtures. The dynamic modulus test of a mixture under uniaxial compression was carried out, and the dynamic modulus master curve of different gradation mixtures was drawn. A mixture's dynamic modulus variation characteristics under different temperatures, loading frequencies, and nominal maximum particle sizes were studied. The main conclusions of this paper are as follows.

(1) At different temperatures and loading frequencies, the dynamical moduli of the three composite-modified oil sludge pyrolysis residue mixtures are consistent, increasing with decreasing temperature and increasing frequency.

(2) There are differences in the decrease in the dynamic modulus of the mixture at different temperatures and loading frequencies. The dynamic modulus decreases slightly at low temperatures, and the dynamic modulus decreases significantly at high temperatures. The dynamic modulus decreases considerably at low frequencies, and the dynamic modulus decreases less at high frequencies.

(3) Based on the time–temperature equivalence principle, the master curve of asphalt mixture with different gradation composite-modified oil sludge pyrolysis residue was established. The master curve of different gradation mixtures is S-shaped, which highly correlates with the test data. In the range of $-10\text{ }^{\circ}\text{C}$ and $54.4\text{ }^{\circ}\text{C}$, the dynamic modulus of asphalt mixture is less affected by frequency and is greatly affected by frequency in the range of $4.4\text{--}37.8\text{ }^{\circ}\text{C}$. The mixture shows strong hysteresis in the moderate frequency range, and the frequency greatly affects the dynamic modulus.

(4) The skeleton structure of the asphalt mixture significantly affects the dynamic modulus. In the low-temperature and high-frequency section, the dynamic modulus of the Sup25 graded mixture is better than that of the other two gradations. Increasing the nominal maximum particle size helps improve the mixture's dynamic modulus. The mixture with a better skeleton structure has the higher dynamic modulus.

Author Contributions: W.R., writing, review and editing. H.Q., writing and conceptualization. X.A. and Y.W., data curation and supervision. S.Z. investigation and visualization. All authors have read and agreed to the published version of the manuscript.

Funding: The research is funded by the grant from the Natural Science Foundation of Xinjiang Autonomous Region (Grant Number: 2022D01C396) and the Technology research and development project of Xinjiang Communications Investment (Group) Co., Ltd. (Grant Number: XJJT-ZKX-FWCG-202301-049).

Data Availability Statement: The data used to support the findings of this study are available from the corresponding author upon request.

Acknowledgments: The research is funded by the grant from the Natural Science Foundation of Xinjiang Autonomous Region (Grant Number: 2022D01C396) and Technology research and development project of Xinjiang Communications Investment (Group) Co., Ltd. (Grant Number: XJJT-ZKX-FWCG-202301-049). The sponsorships are gratefully acknowledged. The contents of this paper reflect the views of the authors and do not necessarily reflect the official views or policies of the sponsors.

Conflicts of Interest: The authors declare no conflict of interest.

References

1. Zhang, L.; Shen, W.; Li, X.; Wang, Y.; Qin, Q.; Lu, X.; Xue, T. Abutment pressure distribution law and support analysis of super large mining height face. *Int. J. Environ. Res. Public Health* **2022**, *20*, 227. [[CrossRef](#)]
2. Li, X.; Zhang, X.; Shen, W.; Zeng, Q.; Chen, P.; Qin, Q.; Li, Z. Research on the mechanism and control technology of coal wall sloughing in the ultra-large mining height working face. *Int. J. Environ. Res. Public Health* **2023**, *20*, 868. [[CrossRef](#)]
3. Zhang, J.; Li, X.; Qin, Q.; Wang, Y.; Gao, X. Study on overlying strata movement patterns and mechanisms in super-large mining height stopes. *Bull. Eng. Geol. Environ.* **2023**, *82*, 142. [[CrossRef](#)]
4. Johnson, O.A.; Affam, A.C. Petroleum sludge treatment and disposal: A review. *Environ. Eng. Res.* **2019**, *24*, 191–201. [[CrossRef](#)]

5. Da Silva, L.J.; Alves, F.C.; de França, F.P. A review of the technological solutions for the treatment of oily sludges from petroleum refineries. *Waste Manag. Res.* **2012**, *30*, 1016–1030. [[CrossRef](#)] [[PubMed](#)]
6. Liu, J.; Jiang, X.; Zhou, L.; Han, X.; Cui, Z. Pyrolysis treatment of oil sludge and model-free kinetics analysis. *J. Hazard. Mater.* **2009**, *161*, 1208–1215. [[CrossRef](#)]
7. Hu, G.; Li, J.; Zhang, X.; Li, Y. Investigation of waste biomass co-pyrolysis with petroleum sludge using a response surface methodology. *J. Environ. Manag.* **2017**, *192*, 234–242. [[CrossRef](#)]
8. Gao, Y.; Yu, Z.; Chen, W.; Yin, Q.; Wu, J.; Wang, W. Recognition of rock materials after high-temperature deterioration based on SEM images via deep learning. *J. Mater. Res. Technol.* **2023**, *25*, 273–284. [[CrossRef](#)]
9. Liu, S.; Li, X. Experimental study on the effect of cold soaking with liquid nitrogen on the coal chemical and microstructural characteristics. *Environ. Sci. Pollut. Res.* **2023**, *30*, 36080–36097. [[CrossRef](#)]
10. Liu, S.; Sun, H.; Zhang, D.; Yang, K.; Wang, D.; Li, X.; Long, K.; Li, Y. Nuclear magnetic resonance study on the influence of liquid nitrogen cold soaking on the pore structure of different coals. *Phys. Fluids* **2023**, *35*, 012009. [[CrossRef](#)]
11. Liu, S.; Sun, H.; Zhang, D.; Yang, K.; Li, X.; Wang, D.; Li, Y. Experimental study of effect of liquid nitrogen cold soaking on coal pore structure and fractal characteristics. *Energy* **2023**, *275*, 127470. [[CrossRef](#)]
12. Seredych, M.; Bandosz, T.J. Sewage sludge as a single precursor for development of composite adsorbents/catalysts. *Chem. Eng. J.* **2007**, *128*, 59–67. [[CrossRef](#)]
13. Zhao, H.; Hou, Y.; Zhu, W.; Zhang, J. Process optimization of preparation adsorbent material and pyrolysis for oily sludge. *Chin. J. Environ. Eng.* **2012**, *6*, 627–632.
14. Wang, C.-Q.; Jin, J.-Z.; Lin, X.-Y.; Xiong, D.-M.; Mei, X.-D. A study on the oil-based drilling cutting pyrolysis residue resource utilization by the exploration and development of shale gas. *Environ. Sci. Pollut. Res.* **2017**, *24*, 17816–17828. [[CrossRef](#)] [[PubMed](#)]
15. Asim, N.; Badiei, M.; Torkashvand, M.; Mohammad, M.; Alghoul, M.A.; Gasaymeh, S.S.; Sopian, K. Wastes from the petroleum industries as sustainable resource materials in construction sectors: Opportunities, limitations, and directions. *J. Clean. Prod.* **2021**, *284*, 125459. [[CrossRef](#)]
16. Vaisman, Y.I.; Pugin, K.G.; Vlasov, A.S. Using the resource potential of drill cuttings in road construction. *IOP Conf. Ser. Earth Environ. Sci.* **2020**, *459*, 022078. [[CrossRef](#)]
17. Mo, W.; Wu, Z.; He, X.; Qiang, W.; Wei, B.; Wei, X.; Wu, Y.; Fan, X.; Ma, F. Functional group characteristics and pyrolysis/combustion performance of fly ashes from Karamay oily sludge based on FT-IR and TG-DTG analyses. *Fuel* **2021**, *296*, 120669. [[CrossRef](#)]
18. Albayati AH, K.; Mohammed, A.M. Effect of Lime Addition Methods on Performance Related Properties of Asphalt Concrete Mixture. *J. Eng.* **2016**, *22*, 120669. [[CrossRef](#)]
19. Zhu, H. Rheological Property of Compound Modification Modified Oil Sludge Asphalt Mortar. Master's Thesis, of Xinjiang University, Ürümqi, China, 2021.
20. Cong, L.; Zheng, X.; Lv, W. Effect of Clay Content in Fine Aggregate on Water Stability of Asphalt Mixture. *J. Tongji Univ. (Nat. Sci.)* **2006**, *34*, 619–623.
21. Birgisson, B.; Soranakom, C.; Napier, J.A.; Roque, R. Microstructure and fracture in asphalt mixtures using a boundary element approach. *J. Mater. Civ. Eng.* **2004**, *16*, 116–121. [[CrossRef](#)]
22. Wu, J.; Liang, J.; Adhikari, S. Dynamic response of concrete pavement structure with asphalt isolating layer under moving loads. *J. Traffic Transp. Eng. (Engl. Ed.)* **2014**, *1*, 439–447. [[CrossRef](#)]
23. Li, Q.; Li, G.; Wang, H. Effect of loading modes on dynamic moduli of asphalt mixtures. *J. Build. Mater.* **2014**, *17*, 816–822.
24. Zhuo, Y.C.; Zhang, J.X.; Zhang, Y.G. Study on Dynamic Modulus of Different Asphalt Mixtures and its Relation with Pavement Performance. *J. China Foreign Highw.* **2021**, *41*, 260–266.
25. Liu, H.; Kong, Y.; Cao, D. Influence of adding polyester fiber on dynamic modulus of asphalt mixture. *J. Highw. Transp. Res. Dev.* **2011**, *28*, 25–29.
26. *JTG E20-2011*; Standard Test Methods of Bitumen and Bituminous Mixtures for Highway Engineering. China Communication Press: Beijing, China, 2011.
27. Wang, F.F.; Yang, P.H.; Yu, T. Study on Catalytic pyrolysis process of oily sludge and analysis of pyrolysis products. *Environ. Eng.* **2019**, *37*, 171–176.
28. *JTG E42-2005*; Test Methods of Aggregate for Highway Engineering. China Communication Press: Beijing, China, 2005.
29. Ran, W.P.; Zhang, S.S.; Zhu, H.L.; Li, L.; Yu, Z. Stability of Asphalt Mortar from Pyrolysis Residue of Oil Sludge Modified with Hydrated Lime Based on Rheological Properties. *China J. Highw. Transp.* **2023**, *36*, 107–119.
30. Gong, B.; Jiang, Y.; Chen, L. Feasibility investigation of the mechanical behavior of methane hydrate-bearing specimens using the multiple failure method. *J. Nat. Gas Sci. Eng.* **2019**, *69*, 102915. [[CrossRef](#)]
31. Cui, W.; Wu, K.; Cai, X.; Tang, H.; Huang, W. Optimizing gradation design for ultra-thin wearing course asphalt. *Materials* **2020**, *13*, 189. [[CrossRef](#)]
32. Gong, B.; Jiang, Y.; Yan, P.; Zhang, S. Discrete element numerical simulation of mechanical properties of methane hydrate-bearing specimen considering deposit angles. *J. Nat. Gas Sci. Eng.* **2020**, *76*, 103182. [[CrossRef](#)]
33. Mohammadi, S.; Mirghaffari, N. A preliminary study of the preparation of porous carbon from oil sludge for water treatment by simple pyrolysis or KOH activation. *New Carbon Mater.* **2015**, *30*, 310–318. [[CrossRef](#)]

34. Lesueur, D.; Petit, J.; Ritter, H.J. The mechanisms of hydrated lime modification of asphalt mixtures: A state-of-the-art review. *Road Mater. Pavement Des.* **2013**, *14*, 1–16. [[CrossRef](#)]
35. Xiong, R.; Qiao, N.; Chu, C. Investigation on low-temperature rheology and adhesion properties of salt-doped asphalt mortars. *J. Jilin Univ. (Eng. Technol. Ed.)* **2020**, *50*, 183–190.
36. Huang, S.C.; Robertson, R.E.; Branthaver, J.F.; Claine Petersen, J. Impact of lime modification of asphalt and freeze–thaw cycling on the asphalt–aggregate interaction and moisture resistance to moisture damage. *J. Mater. Civ. Eng.* **2005**, *17*, 711–718. [[CrossRef](#)]
37. Hu, L.Y.; Zheng, Q.H.; Yu, F.; Chen, J.L.; Luo, R. Master Curve Drawing of Axial Transverse Dynamic Modulus Based on the Same Time-temperature Equivalent Factor. *J. Wuhan Univ. Technol. (Transp. Sci. Eng.)* **2019**, *43*, 146–152.
38. National Cooperative Highway Research Program (NCHRP). *Guide for Mechanistic-Empirical Design of New and Rehabilitated Pavement Structures*; National Cooperative Highway Research Program 1-37 A; NCHRP: Washington, DC, USA, 2004.

Disclaimer/Publisher’s Note: The statements, opinions and data contained in all publications are solely those of the individual author(s) and contributor(s) and not of MDPI and/or the editor(s). MDPI and/or the editor(s) disclaim responsibility for any injury to people or property resulting from any ideas, methods, instructions or products referred to in the content.